HURRICANE IMAGING RADIOMETER WIND SPEED AND RAIN RATE RETRIEVAL: [PART-1] DEVELOPMENT OF AN IMPROVED OCEAN EMISSIVITY MODEL

Salem El-Nimri[1], Linwood Jones[1], Eric Uhlhorn[2], Chris Ruf[3], and Peter Black[4]*

[1] Central Florida Remote Sensing Laboratory
University of Central Florida, Orlando, Florida 32816
U.S.A
* selnimri@mail.ucf.edu
[2] NOAA/AOML/Hurricane Research Division, Miami, Florida, USA
[3] Space Physics Research Laboratory, University of Michigan, Ann Arbor, Michigan
[4] SAIC, Inc at NRL/ Marine Meteorology Division Monterey, California, USA

ABSTRACT

A new microwave radiometric ocean surface emissivity model has been developed to support the analysis and design of the new airborne Hurricane Imaging Radiometer, HIRAD. This radiative transfer model extends current ocean surface emissivity capabilities to higher wind speeds and incidence angles. This model utilizes a variety of empirical data sources many of which were collected in hurricanes.

***Index Terms*—** Hurricane Imaging Radiometer, HIRAD, Stepped Frequency Microwave Radiometer, SFMR, High wind speed, ocean emissivity model

1. INTRODUCTION

Airborne surveillance is crucial for hurricane monitoring because it provides real time update of the hurricane intensity and eye location. The National Oceanic and Atmospheric Administration, NOAA, Hurricane Research Division, HRD, utilizes the Stepped Frequency Microwave Radiometer, SFMR, to provide measurements of the maximum one minute sustain wind speed (the major factor in hurricane category according to the Saffir-Simpson scale). SFMR has been flying on NOAA's WP-3D "hurricane hunter" and USAF WC-130J aircrafts since the late 90's, and it is considered the most reliable surface wind speed measuring instrument in hurricane surveillance. It has demonstrated capability of measuring wind speeds up to 85 m/s (category 5 hurricane), even in the presence of intense rain. SFMR utilizes six different frequencies in the C-band region to perform its measurements.

The Hurricane Imaging Radiometer, HIRAD, is considered a strong candidate for the next generation of hurricane surveillance instrument that could replace SFMR. The HIRAD design combines SFMR multi-frequency C-Band and the Lightweight Rain Radiometer, LRR, image synthesis capabilities in one instrument. It is a four-frequency (4 – 6.6 GHz) synthetic thinned array radiometer that will provide wide swath (3 × the aircraft altitude) that covers the entire eye wall region of a storm in a single pass as shown in Fig. 1. HIRAD is planned to fly on NASA's high altitude "Global Hawk" airplane, that operates at 20 km altitude and provides ~ 70 km swath coverage, which significantly extends the nadir only coverage of SFMR.

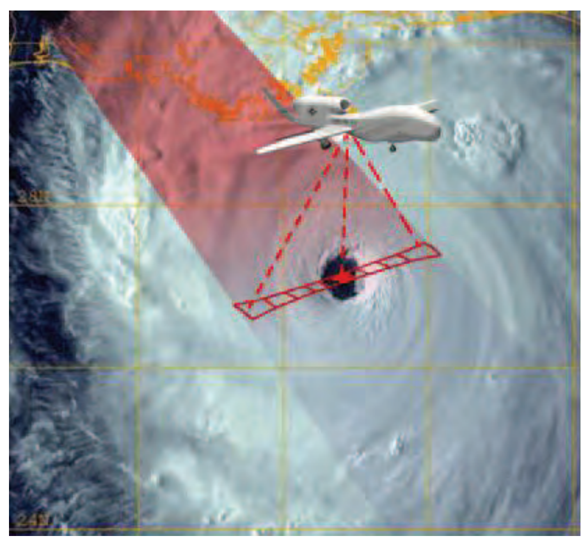

Figure 1 HIRAD wide swath coverage over a hurricane.

2. CFRSL MODEL FORMATION

HIRAD requirements for an ocean surface emissivity model that covers large incidence angles from nadir to > 60 degrees and from moderate to hurricane force high wind speeds (Cat. 5 hurricanes) provides the motivation to develop the CFRSL emissivity model.

Current ocean surface emissivity models are more limited in their range of applicability. For example, the Uhlhorn et. al. [1] model covers the full range of wind speeds up to Cat. 5 hurricanes, yet it is only useful at nadir. Further, the ocean surface emissivity model of Wentz and Meissner [2] is limited to smaller ranges for incidence angle (50 – 60 deg) and wind speed < 20 m/s. Another model by Wilheit [3] fails to track the Uhlhorn surface emissivity at nadir for high wind speeds, and the model of Stogryn [4] also exhibits unrealistic saturation at wind speeds exceeding 45 m/s, whereas SFMR has shown a strong emissivity dependence up to > 85 m/s wind speeds.

Following the approach of Stogryn, the CFRSL ocean surface emissivity (ε_{ocean}) is physically based with empirically turned coefficients that are a linear sum of foam (ε_{foam}) and foam-free sea water (ε_{rough}) emissivities, according to

$$\varepsilon_{ocean} = FF \times \varepsilon_{foam} + (1 - FF) \times \varepsilon_{rough} \tag{1}$$

where FF is the percentage of foam coverage. The foam emissivity is modeled as

$$\varepsilon_{foam} = Q(freq) \times f(ws, EIA) \tag{2}$$

where *Q(freq)* is the empirical frequency dependence and *f(ws, EIA)* is the empirical dependence on wind speed and EIA. Following Stogryn, the foam-free sea water emissivity (ε_{rough}) is

$$\varepsilon_{rough} = \varepsilon_{smooth} + \Delta\varepsilon_{excess} \tag{3}$$

where ε_{smooth} = (1 - Γ) is the smooth surface emissivity, Γ is the Fresnel power reflection coefficient and $\Delta\varepsilon_{excess}$ is the wind induced excess emissivity, given by

$$\Delta\varepsilon_{excess} = g(ws, EIA) \times H(freq, SST) \tag{4}$$

where SST is the sea surface temperature and *g(ws,EIA)* is tuned to SFMR off-nadir T_b measurements and the Miessner and Wentz model extrapolated for ocean emissivity [5]. The term *H (freq,SST)* was unmodified from Stogryn [4].

2.1. Foam Emissivity and Foam Fraction

For high wind speeds, foam becomes the dominant part in the ocean surface emission, so accurate knowledge of the percentage of foam coverage (*FF*), and foam emissivity is required to estimate the total emissivity.

The CFRSL foam emissivity model development was derived iteratively by first assuming *f(ws,EIA=0)* to be equal to 1 at nadir and solving for the frequency dependent part using the Uhlhorn emissivity model. Also it is worth mentioning that the foam free part has a frequency dependence. Uncertainties due to the extrapolation of the foam free part are considered small and negligible at high wind speed. Figure 2 shows the CFRSL foam emissivity with respect to frequency for the range of frequency from L-band to 40 GHz. Also shown are comparisons with Zheng et. al. [6] and Camps et. al. [7] foam measurements at higher and lower frequencies, respectively.

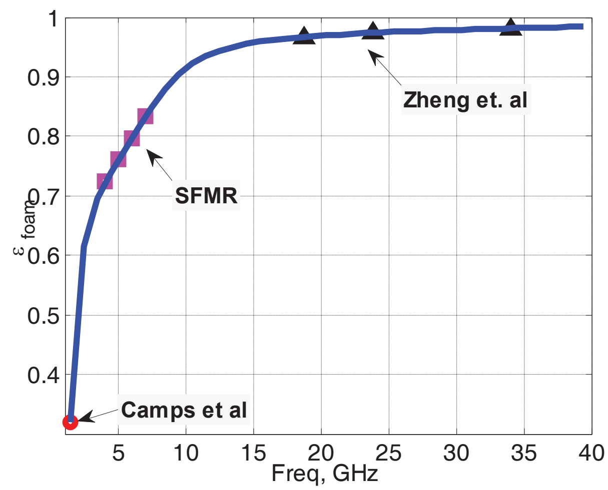

Figure 2 CFRSL foam emissivity with respect to frequency in comparison with Camps et. al. and Zheng et. al.

Next, the dependence of foam fraction (*FF*) on wind speed was derived using the Uhlhorn emissivity model over the dynamic range of wind speed from 7 to 70 m/s. In this calculation, Stogryn's ε_{rough} was used; however, since the function *g(ws,EIA=0)* in (4) was allowed to change, the *FF* was also calculated iteratively.

Equation 5 illustrates the process used in extracting *FF*

$$FF = \frac{\langle \varepsilon_{SFMR} \rangle_{freq} - \langle \varepsilon_{rough} \rangle_{freq}}{\langle \varepsilon_{foam} \rangle_{freq} - \langle \varepsilon_{rough} \rangle_{freq}} \tag{5}$$

where "< >" denote average values. Beyond 70 m/s the model was forced to asymptotically approach a 100% as shown in Fig. 3. Also shown are comparisons with independent data sources for foam white cap coverage (FWC that represents foam only) and foam fraction coverage (FFC that represents foam due to breaking waves and streaks). In this study FFC is our main interest since it represents the total foam (white caps and streaks).

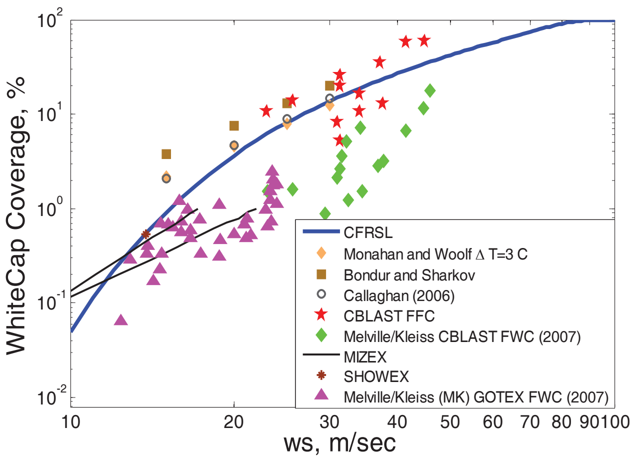

Figure 3 CFRSL foam fraction (*FF*) parameterization with respect to 10-m oceanic wind speed (solid curve) with empirical observations of percentage of sea foam coverage [8-10].

2.2. Wind Speed Coefficient Tuning

To satisfy HIRAD requirements for an emissivity model that is applicable to > 60 deg and over a large range of wind speed, we modeled the foam emissivity as a function of wind speed and incidence angel *f(ws,EIA)*. This functional form of foam emissivity is considered valid based on the findings of Reul and Chapron [11], Zheng et. al. [6]. In the C-Band region, it was proved that foam emissivity varies with thickness of the layer, while this dependence saturates at lower foam thicknesses as frequency increases.
The functional form of this dependence was modeled empirically using data collected from SFMR, WindSat [12], and the Miessner and Wentz emissivity model [2].

SFMR brightness temperatures measurements were collected during the 2003 - 2005 hurricane seasons (listed in Table I). These included measurements at relatively high wind speeds (~ 45 m/s) and off-nadir incidence angles < 35° for horizontal (H-pol) and vertical (V-pol) polarizations that were analyzed to extract the ocean surface emissivity. First, the data were filtered to extract off-nadir measurements during steady aircraft turns, which resulted in a small dataset and reduced the dynamic range of available wind speeds. This occurred because turns were not performed in the eye wall region (maximum winds) due to safety concerns. Next, data were examined for radio frequency interference (RFI) detection, and contaminated SFMR measurements were cleared from the dataset. Because of on-board C-band radars, RFI was experienced on one or more channels approximately 15-25 % of the time. Fortunately, the RFI was relatively easy to detect by relative comparison among SFMR channels using a T_b threshold.

The next step involved "atmospheric clearing" to remove the atmospheric attenuation from SFMR T_b before estimation of the ocean surface emissivity. For this purpose, radiative transfer calculations were performed using a typical hurricane atmosphere by Frank [13]. Further, the effects of rain (emission and attenuation) were removed using the approach of Uhlhorn et al. [14]. Datasets were carefully selected to minimize regions with heavy rain, but typically rain atmospheric clearing was required. This involved estimating the rain rate along the propagation path using SFMR rain retrievals during level flight before and after the turns. For atmospheric clearing, the rain was assumed to be homogeneous with a 100% antenna beam-fill, which is considered to be valid because SFMR operated at low altitudes ~ 2.5 km. Assuming the highest bank being 35 deg this means that the antenna footprint is only displaced by ~ 1.8 km.

Finally, an antenna pattern smoothing bias removal procedure was performed to correct for the large SFMR beam width (16-28 deg).

TABLE I
HURRICANES USED IN HIRAD MODEL DEVELOPMENT

Hurricane	Year	max 1-min sustained wind speed	Number of flights
Fabian	2003	120 kt (60 m/s)	3
Frances	2004	115 kt (58 m/s)	6
Katrina	2005	150 kt (75 m/s)	4
Ophelia	2005	65 kt (34 m/s)	4
Rita	2005	155 kt (78 m/s)	5

SFMR measurements covered the incidence angle range < 35 deg, yet HIRAD geometry required that the model extend > 60 deg. Thus, we used WindSat hurricane analysis results from Ruf. et al. [12] to provide points of reference for the CFRSL model extrapolation. These surface emissivity measurements were not used in the regression, due to concerns related to the large WindSat footprint average (~ 40 km) yet they were used as points of reference at the upper incidence angle range.

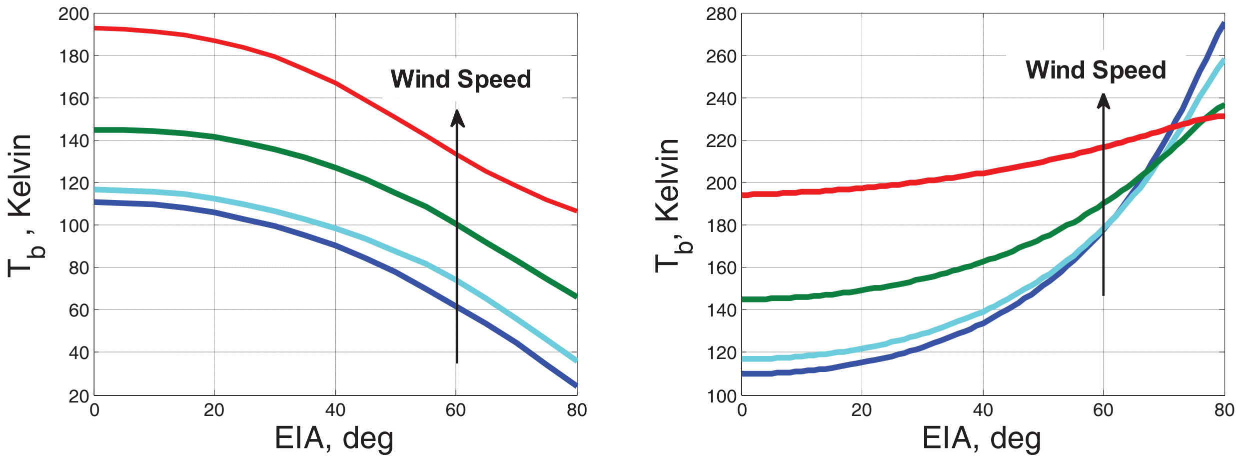

Figure 4 CFRSL surface emissivity model scaled to 300 Kelvin for horizontal polarization (left panel) and vertical polarization (right panel) for 4 GHz, and wind speeds of 6, 20, 40, and 70 m/s.

3. RESULTS

The derived HIRAD ocean surface emissivity model is plotted in Fig. 4 for both horizontal (left panel) and Vertical (right panel) polarizations, at 4 GHz for wind speeds of 6, 20, 40, and 70 m/s. These surface emissivity plots were scaled to 300 Kelvin ($T_b = \varepsilon \times SST$) and extrapolated beyond the 45 m/s (the highest measured ocean surface emissivity from SFMR during aircraft banks). As is noted that as wind speed increases the slops of the emissivity plots for both vertical and horizontal polarizations decreases, yet at a certain wind speed when 100% foam coverage reached, there will be still sensitivity with respect to incidence angle from the H-Pol more than V-Pol, and this is consistent with the observations of Rose. et. al [15].

The validation and comparison with recent SFMR measurements is provided in El-Nimri et. al [16], but additional data from higher banks and higher wind speeds is needed to better tune the model parameters.

4. SUMMARY AND CONCLUSION

This paper gives a brief description of a newly developed ocean surface emissivity model, which extended the current surface emissivity models ranges of capability for higher wind speeds and incidence angles. This model was used in an end-to-end simulation of HIRAD measurements in hurricanes that is described in part-2 of this paper.

5. REFERENCES

[1] Eric W. Uhlhorn, Peter G. Black, James L. Franklin, and Alan S. Goldstein, "Hurricane Surface Wind Measurements from an Operational Stepped Frequency Microwave Radiometer," *American Meteorological Society,* vol. 135, pp. 3070-3085, 2007.

[2] F. Wentz and T. Meissner, "AMSR Ocean Algorithm," Remote Sensing Systems, Santa Rosa, CA November 2 2000.

[3] T. T. Wilheit, "A model for the microwave emissivity of the ocean's surface as a function of wind speed," *IEEE Trans. Gesoci. Electronics,* vol. 17, pp. 244-249, 1979.

[4] A. Stogryn, "The apparent temperature of the sea at microwave frequincies" *IEEE Trans. Antennas Propagat.,* vol. 15, pp. 278-286, 1967.

[5] F. Wentz and T. Meissner, "AMSR Ocean Algorithm " Remote Sensing Systems, Santa Rosa, CA November 2 2000.

[6] Q. A. Zheng, V. Klemas, G. S. Hayne, and N. E. and Huang, "The effect of oceanic whitecaps and foams on pulselimited radar altimeters," *J. Geophys. Res.,* vol. 88, pp. 2571–2578, 1983.

[7] Adriano Camps et. al. "The Emissivity of Foam-Covered Water Surface at L-Band: Theoretical Modeling and Experimental Results From the Frog 2003 Field Experiment," *IEEE Trans. Geoscience and Remote Sensing,* vol. 43, pp. 925-937, 2005.

[8] S. S. Chen, "CBLAST- Hurricane and High-Resolution Fully Coupled Atmosphere-Wave-Ocean Models," in *10th Wave Hindcasting Workshop* Hawaii, 2007.

[9] E. Monahan and D. K. Woolf, "Comments on Variations of Whitecap Coverage with Wind Stress and Water Temperature," *J. Phys. Oceanogr.,* vol. 19, pp. 706-709, 1989.

[10] V. G. Bondur and E. A. Sharkov, "Statistical Properties of Whitecaps on a Rough Sea," *Oceanology,* vol. 22, pp. 274-279, 1982.

[11] N. Reul and B. Chapron, "A model of Sea-Foam Thickness Distribution for Passive Microwave remote Sensing Applications," *Journal of Geophysical research,* vol. 108, pp. 19.1-19.14, 2003.

[12] Chris Ruf, Amanda Mims, and C. Hennon, "The Dependence of the microwave emissivity of the ocean on hurricane force wind speed," in *American Meteorological Society* Orlando, 2007.

[13] W. M. Frank, "The Structure and Energetics of the Tropical Cyclone I. Storm Structure," *Mon. Wea. Rev.,* vol. 105, pp. 1119-1135, 1977.

[14] E. W. Uhlhorn and P. G. Black, "Verification of Remotely Sensed Sea Surface Winds in Hurricanes," *J. Atmos. Oceanic Technol.,* pp. 100-115, Jan. 2003 2003.

[15] L. A. Rose, W. E. Asher, S. C. Reising, P. W. Gaiser, K. M. S. Germain, D. J. Dowgiallo, K. A. Horgan, G. Farquharson, and E. J. Knapp, "Radiometric Measurements of the Microwave Emissivity of Foam " *IEEE Trans. of Geoscience and Remote Sensing,* vol. 40, pp. 2619-2625, December 2002.

[16] S. F. El-Nimri, L. W. Jones, E. W. Uhlhorn, C. S. Ruf, J. W. Johnson, and P. G. Black, "An Improved C-band Ocean Surface Emissivity Model at Hurricane-force Wind Speeds over a Wide Range of Earth Incidence Angles," *GRSL,* 2010.